Natural Hazards
and Earth System
Sciences

Impact of drought hazards on flow regimes in anthropogenically impacted streams: an isotopic perspective on climate stress

Maria Magdalena Warter[1], **Dörthe Tetzlaff**[1,2,4], **Christian Marx**[3], **and Chris Soulsby**[1,3,4]

[1]Department for Ecohydrology and Biogeochemistry, Leibniz Institute of Freshwater Ecology
and Inland Fisheries (IGB), Berlin, Germany
[2]Department of Geography, Humboldt University Berlin, Berlin, Germany
[3]Chair of Water Resources Management and Modeling of Hydrosystems, Technische Universität Berlin, Berlin, Germany
[4]Northern Rivers Institute, School of Geosciences, University of Aberdeen, Aberdeen, UK

Correspondence: Maria Magdalena Warter (maria.warter@igb-berlin.de)

Abstract. Flow regimes are increasingly impacted by more extreme natural hazards of droughts and floods as a result of climate change, compounded by anthropogenic influences in both urban and intensively managed rural catchments. However, the characteristics of sustainable flow regimes that are needed to maintain or restore hydrologic, biogeochemical and ecological functions under rapid global change remain unclear and contested. We conducted an intercomparison of two streams in the Berlin–Brandenburg region of northeast Germany, which are both mesoscale subcatchments of the Spree river: an intermittent rural agricultural stream (the Demnitzer Millcreek) and a heavily anthropogenically impacted urban stream (the Panke). Through tracer-based analyses using stable water isotopes, we identified the dominant physical processes (runoff sources, flowpaths and age characteristics) sustaining streamflow over multiple years (2018–2023), including three major drought years (2018–2020, 2021–2022). In the urban stream, low flows are regulated through artificially increased baseflow from treated wastewater effluents (by up to 80 %), whilst storm drainage drives rapid, transient high-flow and runoff responses (up to 80 %) to intense convective summer rainfall. The intermittent groundwater-dominated rural stream experienced extended no-flow periods during drought years (∼ 60 % of the year) and only moderate storm runoff coefficients (< 10 %) in winter along near-surface flow paths after heavy rainfall. In both streams, groundwater dominance with young water influence prevails, with low water ages in the urban stream (< 10 %) despite significant urban runoff and higher ones in the rural stream (∼ 15 %). Urban cover resulted in a mean transit time of ∼ 4 years compared to arable land at ∼ 3 years, highlighting the interlinkages of land use and catchment properties on catchment transit times. Understanding seasonal and interannual variability in streamflow generation through a tracer-based hydrological template has the potential to assess the impacts of natural hazards on the sustainability of future baseflow management, including wider water quality and ecological implications across anthropogenically impacted environments.

1 Introduction

Urbanization and anthropogenic alterations to hydrological pathways, drainage networks and flow regimes have progressively changed the water balance and dynamics of contemporary streams and rivers, increasing their sensitivity and impacts to climatological and hydro-meteorological hazards (Bonneau et al., 2018; Soulsby et al., 2014; Stewardson et al., 2017). Along with the well-established impacts of anthropic changes imposed on urban freshwater, many other areas, including peri-urban and rural agricultural environments, are also experiencing dramatic alterations to natural flow regimes and hydrologic processes due to increase drought frequency and intensity (Döll and Schmied, 2012; Yang et al., 2011). These changes are propagated by the persistent reorganization of surface and subsurface hydrological flowpaths, widespread land use changes and stream net-

work alterations, as well as increasing baseflow manipulations (Bonneau et al., 2018; Marx et al., 2021; Oswald et al., 2023; Soulsby et al., 2014).

In recent years the frequency and intensity of hazards such as floods and severe multiyear droughts have contributed to a paradigm shift in future streamflow management needs and the recognition of a persistent lack of understanding of essential hydrologic processes in urban and other anthropogenically impacted systems (Arthington et al., 2006; Oswald et al., 2023). Despite the importance of natural flow variability (Poff et al., 1997; Stewardson et al., 2017) and numerous studies demonstrating the effects of changes in natural flow regimes on hydrological and ecological functions (Arthington et al., 2006; Bhaskar et al., 2016; Olden and Poff, 2003; Poff and Zimmerman, 2010; Tetzlaff et al., 2005), there is still a distinct lack of understanding of anthropogenically impacted flow regimes and their evolution in the face of rapid global change. This provides a weak evidence base for managers wanting to maintain or restore a baseline of natural flow regime characteristics that supports the hydrologic, biogeochemical and ecological functionality of freshwater systems that provide important ecosystem services (Acreman et al., 2014; Arthington et al., 2006).

Concerns over water stress and drought as drivers of rapid hydrological change have intensified both in cities (Kuhlemann et al., 2020; Paton et al., 2021) and lowland agricultural catchments (Kleine et al., 2021a; O'Briain, 2019; Wu et al., 2021). During recent severe drought years (2018–2020) in northern and central Europe, significant shifts in streamflow from perennial to intermittent were widely observed, with the probability and longevity of intermittency likely to increase with projected increases in temperatures across Europe (Kleine et al., 2020; Lobanova et al., 2018; Sarremejane et al., 2022; Tramblay et al., 2021). In addition, ongoing urban densification contributes to increasingly flashy hydrographs, deteriorating water quality and increased influence of wastewater discharges, causing flow regimes to increasingly deviate from the "natural flow paradigm" with a seasonal succession of high and low flows (Bhaskar et al., 2016; Bonneau et al., 2018; Marx et al., 2021; Soulsby et al., 2015). Especially biodiversity and the health of aquatic and wetland ecosystems hinge on ecological processes which are dependent on the natural occurrence of and variability in high and low flows, while baseflows exert critical controls on habitat maintenance and the survival of different aquatic species, as well as the moderation of water temperatures, water quality, oxygen levels, nutrient loads and vegetation growth (Arthington et al., 2006; Poff and Zimmerman, 2010; Stewardson et al., 2017).

For stream management, a landscape-scale understanding of controls on streamflow regimes requires an integrative approach that captures ecologically and hydrological meaningful characteristics of seasonal flow dynamics (Arthington et al., 2006; Tetzlaff et al., 2005; Tonkin et al., 2021). Environmental tracers, such as stable water isotopes, can be use-

ful for characterizing complex hydrological systems in order to understand hydrological functioning across multiple scales (Ehleringer et al., 2016; Jasechko, 2019; Kendall and McDonnell, 1998; Stevenson et al., 2022). Tracer applications and tracer-based models can provide insight into controls on streamflow generation across different climatic and geographic scales (Bonneau et al., 2018; Von Freyberg et al., 2018; Stevenson et al., 2022). The conservative behavior of stable water isotope ratios of water (δ^{18}O, δ^2H) and their ability to integrate hydrological processes make them useful indicators of water sources and flowpaths (Ehleringer et al., 2016; Von Freyberg et al., 2018; Marx et al., 2021). This can help quantify drought effects (Kleine et al., 2020; Kuhlemann et al., 2020; Smith et al., 2020b), mean transit times and water ages (Birkel et al., 2016; Hrachowitz et al., 2010; Soulsby et al., 2015; Tetzlaff et al., 2015), as well as groundwater–surface-water interactions and recharge (Wallace et al., 2021; Ying et al., 2024), across a range of temporal and spatial scales.

As streamflow generation and intermittency is becoming an increasingly important issue under advancing climate change in the Berlin–Brandenburg region (Kleine et al., 2021; Luo et al., 2024; Ying et al., 2024), a more integrated understanding of a catchment's ability to capture and release water is invaluable. We focus on two contrasting catchments – one urbanized and one rural agricultural catchment, both within the Berlin–Brandenburg region. Both catchments are tributaries of the Spree river, which serves as a major water provider to the city of Berlin and experienced extreme hydroclimatic conditions between 2018–2020, including a major drought period (Creutzfeldt et al., 2021). Using a long-term dataset of daily stable water isotopes and hydrological analyses of discharge dynamics, we sought to understand how drought and intensive storm events have influenced the hydrological and physical functioning of streamflow regimes in two contrasting anthropogenically impacted catchments.

We specifically aim to (i) assess how hydrological functioning such as water partitioning, runoff sources, transit times and water ages varies between two contrasting catchments over a 5-year period; (ii) characterize streamflow persistence and resilience during the extreme drought period of 2018–2020 and in response to selected intensive storm events as exemplary hazards; and (iii) understand implications for flow regime changes under projected future hydroclimate perturbations. We focused on characterizing the contrasting streamflow responses between urban systems with large urban storm drain effects and artificially increased baseflow vs. rural groundwater-fed intermittent systems with agricultural drainage within the Berlin–Brandenburg region, where drought hazards affect the availability and distribution of freshwater. In doing so, we sought to provide the hydrological context and evidence basis to support environmental decision-makers in establishing sustainable environmental flow targets that maintain biodiversity and ecological integrity (Poff and Zimmerman, 2010; Tonkin et al., 2021).

2 Study catchments

In this study, Demnitzer Millcreek – a rural agriculturally influenced stream in the state of Brandenburg – and the Panke river – a heavily urbanized stream in Berlin – were compared (Fig. 1). Both catchments (hereafter referred to as the rural and urban catchments) are situated within 100 km of each other and are tributaries of the Spree river, which has a catchment size of $> 10\,000\,\text{km}^2$ and is the major water provider to the city of Berlin. Both catchments are situated in one of the driest parts of northeast Germany with 577 mm of annual precipitation (1981–2010 average) distributed throughout the year as frequent, lower-intensity frontal winter rains and infrequent heavy convective storms in summer (DWD, 2019). However, regional climate differences exist between the dense urban metropolitan area of Berlin and the drier lowland Brandenburg region, where potential evapotranspiration generally exceeds annual precipitation inputs, thus increasing drought sensitivity ($\sim 700\,\text{mm}\,\text{yr}^{-1}$) (DWD, 2023).

The rural catchment (total catchment area $\sim 66\,\text{km}^2$) is strongly influenced by the regional groundwater system of the Spree valley. The catchment has a mixed land use, including forest, wetland, cereal crops and pastures, with only small, distributed villages giving a 2 % urbanized area (Fig. 1b). A full table of land use distribution for both catchments is provided in the Supplement (Table S1). The site is part of a long-term ecohydrological observatory, and extensive meteorological and ecohydrological data have been measured at multiple temporal and spatial scales since 2018 (Tetzlaff et al., 2023). Arable non-irrigated land use is highest in the northern part of the catchment ($\sim 68\,\%$). Agricultural crops primarily include water-demanding cereal crops, such as winter wheat, barley and maize, occupying the higher-quality soils, whereas in the lower part of the catchment mixed forest and wetlands dominate, which are primarily used as pastureland (Fig. 1d) (Smith et al., 2021).

As the topography is flat and characteristic of a lowland landscape, elevation gradients are negligible across the catchment. This reflects the strong influence of glaciation, resulting in characteristic sections of unmixed sediments. While soils in the agricultural areas comprise silty brown earths, the lower catchment is dominated by sandy soils with low water retention. The river channel network is fringed by peaty soil, particularly in the central wetlands (Fig. 1f). The upper catchment is underlain by unconsolidated sediments of a ground moraine, with a moderately permeable unconfined aquifer and shallow groundwater levels within a few meters of the surface (Fig. 1f) (Ying et al., 2024). The stream network has been significantly altered by historical agricultural management, resulting in a high density of drainage ditches and artificial channels that affect nutrient transport and water quality. To increase nutrient retention and regulate water quality, a nature-based solution was adopted by restoring the central wetlands by partially blocking drains (starting in 2000), installing a weir and shallow-

ing wetland channels, which increased the water retention in the area and led to a subsequent recolonization by beavers (around 2007) (Smith et al., 2020a). The rural catchment is highly drought-sensitive, with an intermittent groundwater-dominated flow regime (with the stream being dry most years for 3–4 months) and overall low runoff coefficients even during wet periods ($< 10\,\%$) due to high evaporative losses (Kleine et al., 2020). Groundwater recharge primarily occurs during the cold and wet season, driving seasonal streamflow generation.

The urban catchment ($\sim 220\,\text{km}^2$) is drained by the highly regulated Panke river, also a tributary of the Spree, draining a densely urbanized landscape (Fig. 1c). The headwaters are predominantly rural, lying on the northern edge of the Warsaw–Berlin glacial spillway. The main geological unit of the shallow aquifer (AQ1) that feeds the catchment is partially confined in the east by an overlying ground moraine and unconfined in the lower catchment with layers of sands and gravels overlying an aquitard of glacial till (Fig. 1g). Like the rural catchment, the stream network drains silty soils in the headwaters and sandy soils in the south. While in the north of the catchment $\sim 22\,\%$ is covered by urban fabric (see Table S1 in the Supplement), the lower catchment is more densely urbanized ($\sim 40\,\%$). Upstream, streamflow is generally groundwater-dominated, with seasonally varying inflows from agricultural and forested areas, in addition to the impact of urban storm drains, with some stretches of the river dry in summer (Marx et al., 2021) (Fig. 1e). In the lower catchment the dominant sources of runoff are effluent releases, which generally vary in response to season but are an increased volume of wastewater flowing into the river (up to 80 %) during the drier summer periods to enhance baseflow. Conversely, during wetter periods and in the case of heavy summer storm events, peak flows are diverted into the neighboring Tegeler catchment and the Nordgraben (Marx et al., 2023). This has led to a highly artificial flow regime with no clear seasonal variation between high and low flows. In recent years the catchment has been subjected to targeted stream restoration to improve ecological conditions and water quality, as well as flood mitigation by rainwater management (SenUVK, 2009). The urban catchment, while different in size, land use, geology and water management, did resemble the rural catchment prior to the advanced urbanization and loss of agricultural and forest area (Kleine et al., 2020, 2021b; Marx et al., 2023). Therefore, the comparison between both catchments elucidates baseflow responses following anthropogenic impact and extensive management.

3 Data and methods

3.1 Climate and hydrological data

In the rural catchment, hourly meteorological data were obtained for the period 2018–2023 from automatic weather
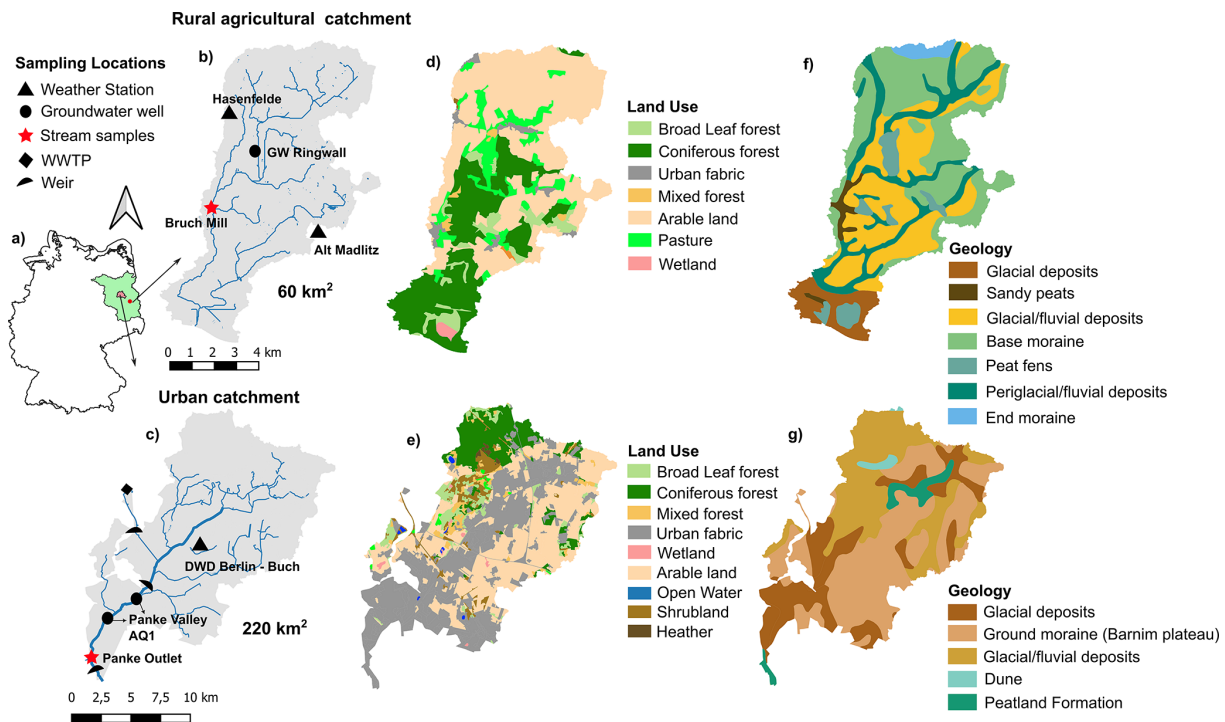
Figure 1. (a) Location of catchments within the Berlin–Brandenburg region. **(b, c)** Overview of sampling locations in the rural and urban catchments, respectively, including stream sampling locations (red) of regular stream isotopic samples, groundwater monitoring wells, weather stations and stream weirs. **(d, e)** Distribution of land use. **(f, g)** Map of the geology in both catchments. (Base maps: LGB (Landesvermessung und Geobasisinformation Brandenburg), 2020; Umweltatlas Berlin/ALKIS, 2020.)

stations (AWSs) at locations in Hasenfelde (WLV, Environmental Measurement Limited, UK) and Alt Madlitz (Campbell Scientific, USA) (Fig. 1b). A 15 min discharge was measured at Bruch Mill (catchment area: $42\,\mathrm{km^2}$) from water level measurements by pressure sensors (AquiLite ATP 10, AquiTronic Umweltmeßtechnik GmbH, Kirchheim/Teck, Germany) and transformed through an established rating curve (Smith et al., 2020b). Hourly meteorological data (2018–2023) for the urban catchment were obtained from a climate station (Buch) of the German Weather Service (DWD, 2023) (Fig. 1c). Daily and 15 min discharge data were obtained for a station in the lower Panke catchment (Bürgerpark). Both weather stations have been previously used in studies of each catchment (Kleine et al., 2020, 2021b; Marx et al., 2023). Groundwater levels in the urban catchment were taken from wells in the unconfined Panketal aquifer (AQ1), provided as publicly available data from the Berlin Senate (SenUVK, 2023). Groundwater in the rural catchment was monitored from a location in a forest in the central catchment (GW Ringwall, screened 2–4 m below surface), with groundwater levels logged every 4 h (AquiLite ATP10, AquiTronic Umweltmeßtechnik, GmbH, Kirchheim/Teck, Germany).

Hydrological and climate data were separated into hydrological water years (WYs) (1 October–30 September), which were used to calculate different metrics for each stream, such

as total runoff (Q_{Ro}), storm totals and intensity, storm duration, and annual and seasonal precipitation totals and magnitudes (minimum, maximum) of discharge (see Table S2 for a summary of parameters). Discharge was normalized to catchment areas (urban: $220\,\mathrm{km^2}$; rural $42\,\mathrm{km^2}$), and flow duration and double-mass curves were derived to characterize interannual variability in discharge responses. The hydrograph separation of stream discharge into baseflow (Q_{B}) and stormflow (Q_{S}) was achieved using HydRun, a MATLAB-based toolbox (Tang and Carey, 2017), which is based on a recursive digital filter technique developed by Nathan and McMahon (1990). The filter coefficients (fc) and number of filter passes ranged between 0.7–0.99 and 0–10, respectively. Flashiness, as the rate of change in streamflow, was estimated through the Richards–Baker flashiness index (Baker et al., 2004) using daily stormflow data.

Hourly precipitation was used to characterize total event precipitation (P_{total}, mm), mean precipitation intensity (P_{int}, $\mathrm{mm\,h^{-1}}$), streamflow peak (Q_{peak}, $\mathrm{L\,s^{-1}\,km^{-2}}$), maximum precipitation over 1 h (P_{max}, $\mathrm{mm\,h^{-1}}$) and rainfall duration (T, hours). Storm events were identified automatically, whereby precipitation events exceeding 1 h were aggregated; for multiple consecutive events with $< 5\,\mathrm{h}$ breaks or multi-day events, the event precipitation was summarized into one total storm amount. Statistical differences in storm characteristics were assessed through Kolmogorov–Smirnov tests

and Spearman rank correlations using a p threshold of at least 0.05 (95 % confidence level). The annual runoff coefficient was calculated as the ratio between stormflow and precipitation using annual runoff and total annual precipitation (Q_{Ro}/P), while total annual runoff was estimated using annual discharge and baseflow totals ($Q_{Ro} = Q_S - Q_B$). The baseflow index (BFI) was calculated as a ratio of the total baseflow volume to the total runoff volume for each hydrological year to assess the proportion of stream runoff derived from stored sources (e.g., groundwater).

3.2 Stable water isotopes

Daily precipitation isotopes were collected at Hasenfelde (rural) from 2018 and at the Steglitz Urban Ecohydrological Observatory (SUEO) (urban) in southeast Berlin from 2019 using modified ISCO 3700 (Teledyne ISCO, Lincoln, USA) automated samplers. Samples were protected from evaporation by a paraffin layer (thickness > 0.5 mm; IAEA/GNIP precipitation sampling guide V2.02 September 2014). At Bruch Mill (rural), daily stream water isotopes were sampled from 2018 at 16:00 LT each day using an automated ISCO 3700 (also protected from evaporation by paraffin). In the urban catchment, daily stable water isotope samples were collected manually from October 2019 until December 2022, as well as weekly isotopes from 2023 onwards, near the most downstream gauging station (Fig. 1c). Monthly groundwater isotope samples were collected from multiple wells in the AQ1 aquifer as part of a measurement campaign in 2020/2021 (Marx et al., 2021). All samples were filtered (0.2 μm cellulose acetate) into 1.5 mL vials and analyzed for $\delta^{18}O$ and δ^2H using a Picarro L2130-i cavity ring-down water isotope analyzer (Picarro Inc., Santa Clara, CA, USA) in reference to the Vienna Standard Mean Ocean Water (VSMOW). Relationships between daily discharge and stream water isotopes were assessed using Kolmogorov–Smirnov and Spearman rank correlation coefficients.

Local meteoric water lines (LMWLs) were derived using daily precipitation isotope values from Steglitz (February 2019–September 2023) and Hasenfelde (July 2018–July 2023) for the urban and rural catchments, respectively, by weighting respective precipitation inputs. To assess evaporation effects on stream water isotopic composition we also calculated the line-conditioned excess (lc-excess), which defines residuals from the LMWLs (Landwehr and Coplen, 2006). For each catchment, lc-excess was estimated for urban as

$$\text{lcexc} = \delta^2H - 7.8 \cdot \delta^{18}O - 7.1 \, (R^2 = 0.98, \, p < 0.001), \quad (1)$$

and for rural as

$$\text{lcexc} = \delta^2H - 7.68 \cdot \delta^{18}O$$
$$- 7.68 \, \left(R^2 = 0.98, \, p < 0.001\right). \quad (2)$$

3.3 Water ages and mean transit time estimations

To assess the fraction of stream water that fell as recent precipitation and use it as a metric of the age of stream water, young water contributions (F_{yw}) were estimated using the open-access code of von Freyberg et al. (2018). This is based on an iteratively re-weighted least squares (IRLS)-fitted sine-wave method using observed precipitation and stream water isotopes to estimate the fraction of stream water that fell as precipitation within the previous 2–3 months as an indicator of catchment function. We compared sine-wave fitting amplitudes of daily amounts of weighted precipitation δ^2H and $\delta^{18}O$ to stream water isotopes in both streams. For simplicity only results for $\delta^{18}O$ are shown in subsequent plots.

For intercomparison between the rural and urban stream functioning, mean transit times (MTTs) were estimated as another metric of hydrologic response. We used daily amount-weighted precipitation isotope data from SUEO (urban) and AWS Hasenfelde (rural) and daily stream water isotopes and applied two different lumped convolution integral models – the three-parameter two-parallel linear reservoir (TPLR) model (Weiler et al., 2003) and the two-parameter gamma model (Hrachowitz et al., 2010) – to estimate transit time distributions (TTDs) (see Table S3 for details). The TPLR model accounts for fast- (τ_f) and slow-flow reservoirs (τ_s), approximating younger and older water contributions. The reservoirs are partitioned by the φ parameter, ranging from 0–1, which separates the rapid and slow responding flows from surface and subsurface sources. In the urban area we based φ on the percentage of impervious areas that drive fast urban drainage to the stream. In the rural catchment we used non-irrigated arable land area, as rapid runoff is more likely contributed due to more compacted soils and agricultural drainage networks.

The gamma model is defined by the shape parameter α (–) and the scale parameter β (days), with the MTT calculated as the product of the two. The parameter ranges for the TPLR (τ_f, τ_s) and gamma model (α, β) were sampled from predefined parameter ranges using Monte Carlo realizations in order to find the best fit estimates. To avoid the influence of evaporative fractionation on model estimates, a lc-excess filter was applied to stream water isotopes, whereby samples with strong evaporative fractionation were excluded from calibration. We used different lc-excess filters for urban and rural streams (rural: lc-excess < −2.5‰ (i.e., more enriched); urban: lc-excess < −4‰ (more depleted)), as greater evaporative fractionation effects were observed in the rural stream. Model fits were assessed using Nash–Sutcliffe efficiency (NSE) (Nash and Sutcliffe, 1970), root mean square error (RMSE) and coefficient of determination (R^2). Due to the limitations of the stable water isotopes to detect transit times longer than 5 years (Stewart et al., 2010), the scale parameter β of the gamma model and the τ_s parameter in the TPLR model were limited to 1825 d.

4 Results

4.1 Rainfall-runoff characteristics and storm responses

The sampling period (2018–2023) was strongly marked by the intensive drought between 2018–2020, resulting in below-average precipitation and marked discharge responses in both catchments. Annual discharge statistics for both catchments were summarized for each hydrological year in Table 1. During WYs 2019–2020 and 2021–2022 precipitation totals in the Brandenburg region were $\sim 20\%$–30% below the long-term average, while in the metropolitan area they were reduced by $\sim 10\%$–20%. Several heavy convectional rainstorms during the summers of 2021 and 2023 resulted in above-average annual totals and distinct discharge responses in both catchments. However, regional differences become apparent most notably during summer 2019, when a large convectional event over Berlin produced almost $46\,\mathrm{mm\,h^{-1}}$ and an urban discharge peak of $5.3\,\mathrm{L\,s^{-1}\,km^{-2}}$ (Fig. 2c, d), while in rural Brandenburg no rain was recorded during the same period. The extremely sandy soil of the rural catchment and large soil moisture deficits generally limited streamflow response to summer storm events despite the size and intensity of some of events (i.e., June 2021) (Fig. 2a, b). Only minimal transient flow or very small streamflow peaks (i.e., summer 2020) were detected, likely originating from saturated areas fringing the channel bed or the wetter riparian areas upstream and receding quickly to isolated pools of water, whereas significant discharge responses could be seen in the urban stream (Fig. 2d). This is in line with a noted strong positive correlation between storm discharge (Q_S) and total event precipitation ($R^2 = 0.54$, $p < 0.0001$) in the urban stream, which was less evident in the rural stream ($R^2 = 0.18$, $p < 0.001$).

Due to the nature of the urban catchment functioning and management, distinct and large step changes with differences of up to $10\,\mathrm{L\,s^{-1}\,km^{-2}}$ were also observed following the most intense events. Hydrograph separation showed that the large streamflow peaks after events typically subsided within $< 1\,\mathrm{h}$. Conversely during low-flow and drought periods, step changes by up to $1\,\mathrm{m^3\,s^{-1}}$ (from 0.2 to $0.6\,\mathrm{L\,s^{-1}\,km^{-2}}$) could be observed (i.e., April 2020), a clear response to the additional discharge of wastewater. Characteristic of such intensely managed urban streams, a higher specific discharge was observed compared to the rural stream, with mean daily discharge ranging between 0.2–$0.45\,\mathrm{L\,s^{-1}\,km^2}$ and peak flows of up to $3.4\,\mathrm{L\,s^{-1}\,km^2}$ (Fig. 2d). This is a clear effect of urban water management, keeping baseflow at a minimum level ($\sim 0.29\,\mathrm{L\,s^{-1}\,km^2}$) through the consistent influence of wastewater, which contributed up to 80% of annual discharge. In contrast, the rural stream was characterized by clear seasonal intermittency, with the onset of the flowing and fully connected phase strongly tied to the onset of autumn and winter rainfall and increasing groundwater levels. The lack of management and additional water sources to increase streamflow in the rural catchment resulted in relatively low mean discharge rates ($0.15\,\mathrm{L\,s^{-1}\,km^2}$), with groundwater supporting 50%–70% of baseflow (BFI: 0.5–0.7; Table 1). High flows could reach up to $0.5\,\mathrm{L\,s^{-1}\,km^2}$ (i.e., in spring 2022), which is consistent with elevated groundwater levels during the same winter and spring period (Fig. 2b).

While annual runoff was characteristically low in the rural catchment, with runoff coefficients between 0.1 and 0.26 (Table 1), owing to the high evapotranspiration (up to 80%), they were distinctly higher in the urban catchment (0.8–1.5), generally exceeding the annual precipitation input and thus reflecting the substantial water subsidy from wastewater effluents and interbasin water transfers. Water abstraction occurs in the catchment to support the city's water supply, with large amounts of water imported through interbasin water transfers (from the Spree and Havel) from bank filtration. Groundwater levels in the rural catchment showed strong seasonality, with relatively shallow depths of around $2.4\,\mathrm{m\,b.g.l.}$ ($\pm 0.3\,\mathrm{m}$) and the highest levels in April and the lowest in autumn. A slight trend in recovery has been noted in 2022 and 2023 following a wetter year (see Fig. S1). As part of the Barnim aquifer, groundwater in the confined urban aquifer was also relatively shallow (2–3 m b.g.l.), showing only minimal seasonal variability but a notable overall decline in summer levels in recent years due to a lack of winter recharge.

4.2 Differences in seasonal flow regimes

Annual flow duration curves (FDCs) and double-mass curves clearly illustrated the different catchment sensitivities of high- and low-flow conditions to cumulative annual precipitation and hydroclimate (Fig. 3a, b). In the rural stream, the higher slope of flow duration curves highlighted its intermittent nature and low-baseflow component, with most years showing zero flow periods for an average of 60% of the year. The effects of the drought are reflected in the flat FDCs of WYs 2018–2019 and 2019–2020, where low- or no-flow conditions (Q_{95}) were exceeded almost 70% of the year and double-mass curves show the lack of response in streamflow. In contrast, high-flow conditions (Q_5) were greatest during 2022–2023 following a wet spring, and flows continued for almost 65% of the time. The mean flashiness index for the rural stream was relatively low at 0.07 (Table 1). In the rural catchment, the imbalance between annual discharge and precipitation becomes evident, with the majority of annual precipitation lost to the high evaporative demand ($\sim 80\%$), as seen in the low runoff coefficients (Table 2).

In contrast, the effect of urban water management on seasonal streamflow generation becomes apparent in the urban stream, with cumulative discharge often exceeding cumulative annual precipitation (Fig. 3b) due to additional inflow of water from sources outside the catchment. The higher discharge variability and stronger baseflow component, as well as marked responses to precipitation events as evi-

Nat. Hazards Earth Syst. Sci., 24, 3907–3924, 2024

https://doi.org/10.5194/nhess-24-3907-2024

Table 1. Summarized annual discharge statistics for the rural and urban streams per water year; total annual precipitation (mm), specific discharge (Q_{mean}), maximum and minimum daily discharge (Q_{max}, Q_{min}) (all in $L\,s^{-1}\,km^{-2}$), and the 95th and 5th discharge percentiles (Q_{95}, Q_5), as well as total annual runoff (Q_{Ro} in mm), annual baseflow index (BFI) and annual runoff coefficient (Q/P).

Water year	Annual P (mm per WY)	Q_{max} ($L\,s^{-1}\,km^{-2}$)	Q_{min} ($L\,s^{-1}\,km^{-2}$)	Q_{mean} ($L\,s^{-1}\,km^{-2}$)	Q_5 ($L\,s^{-1}\,km^{-2}$)	Q_{95} ($L\,s^{-1}\,km^{-2}$)	Q_{Ro} (mm per WY)	BFI (–)	Q/P (–)
Rural									
2019	388.6	0.23	0	0.01	0.06	< 0.01	44.6	0.54	0.11
2020	494.4	0.34	0	0.03	0.13	< 0.01	52.5	0.72	0.11
2021	534.8	0.42	0	0.06	0.18	< 0.01	133.7	0.58	0.25
2022	434.1	0.40	0	0.06	0.18	< 0.01	113.1	0.64	0.26
2023	535.2	0.48	0	0.05	0.22	< 0.01	115.3	0.56	0.22
Urban									
2019	546.4	0.75	0.16	0.45	0.70	0.2	819.4	0.76	1.49
2020	527	0.64	0.01	0.27	0.54	0.07	670.5	0.72	1.27
2021	600.5	0.73	0.16	0.45	0.67	0.19	872.8	0.78	1.45
2022	461.4	0.9	0.1	0.35	0.65	0.14	447.4	0.86	0.96
2023	624.0	0.76	0.02	0.33	0.62	0.165	523.0	0.82	0.84

Table 2. Young water fractions over the entire study period and per water year for the rural and urban streams obtained from sine-wave fitting, including coefficient of determination (R^2), p value and residual standard errors over the entire study period.

WY	$\delta^{18}O$ rural				$\delta^{18}O$ urban			
	F_{yw}	R^2_{adj}	p value	RSE	F_{yw}	R^2_{adj}	p value	RSE
2019	0.37	0.83	< 0.001	0.14	–	–	–	–
2020	0.22	0.70	< 0.001	0.25	0.12	0.35	< 0.001	0.22
2021	0.09	0.58	< 0.001	0.17	0.05	0.05	0.0002	0.33
2022	0.24	0.62	< 0.001	0.15	0.05	0.08	< 0.001	0.23
2023	0.28	0.37	< 0.001	0.23	0.15	0.21	0.0002	0.24

denced also in the runoff coefficients (Table 1), were visible in the individual FDCs. Similar to the rural stream, the effects of the drought became most evident in WY 2019 and WY 2021, as low flows ($< Q_{95}$) were uncharacteristically high due to additional contributions of increased effluent discharge, resulting in observed higher annual baseflow ($Q_B \sim 0.35\,L\,s^{-1}\,km^{-2}$). The flashy streamflow responses to summer convectional events during WYs 2022 and 2023 were also visible in the steeper curves of the medium flow segment (0.2–0.7 flow exceedance probabilities), while the flatter mid-segment in WY 2020 hints at a more sustained groundwater flow contribution (Fig. 3a), corresponding to the increased groundwater levels observed in the Panketal aquifer (AQ1.2) in those years (see Fig. S2).

Relationships between daily isotopic variations (indexed by $\delta^{18}O$) and specific discharge provide further evidence of time-variant source contributions to streamflow in each catchment (Fig. 4b, c). While in the rural stream $\delta^{18}O$ showed a positive correlation with discharge ($r = 0.41$, $p < 0.01$), despite overall modest variations in daily $\delta^{18}O$ (SD = 0.6‰), in the urban stream, $\delta^{18}O$ and discharge were negatively correlated ($r = -0.25$, $p < 0.01$) with a clear sea-

sonal distinction between high flows in winter and low flows in summer (Fig. 2d). The intermittent streamflow regime of the rural stream and marked seasonality in stable water isotopes illustrated the time-variant contributions from mixed sources (e.g., precipitation and groundwater) during winter and spring flow periods, while in summer, as streamflow starts to decline, the remaining stream water was increasingly subject to evaporative fractionation effects. Particularly as groundwater levels recede and the channel network becomes disconnected, only isolated open-water surfaces remain in the streambed, which are affected by evaporative fractionation (Fig. 2b).

4.3 Spatial variability in precipitation and streamflow isotopes

The isotopic signatures of rainfall in both catchments were highly seasonal (rural: mean $\delta^{18}O = -6.03$‰, SD = 3.27‰ and mean $\delta^2H = -42.12$‰, SD = 21.59‰; urban: mean $\delta^{18}O = -6.09$‰, SD = 3.15‰ and mean $\delta^2H = -42.11$‰, SD = 21.97‰), with rainfall being more depleted in winter and more enriched in summer (Fig. 2a, c). As a general interpretation, the closer together the values are, the less vari-
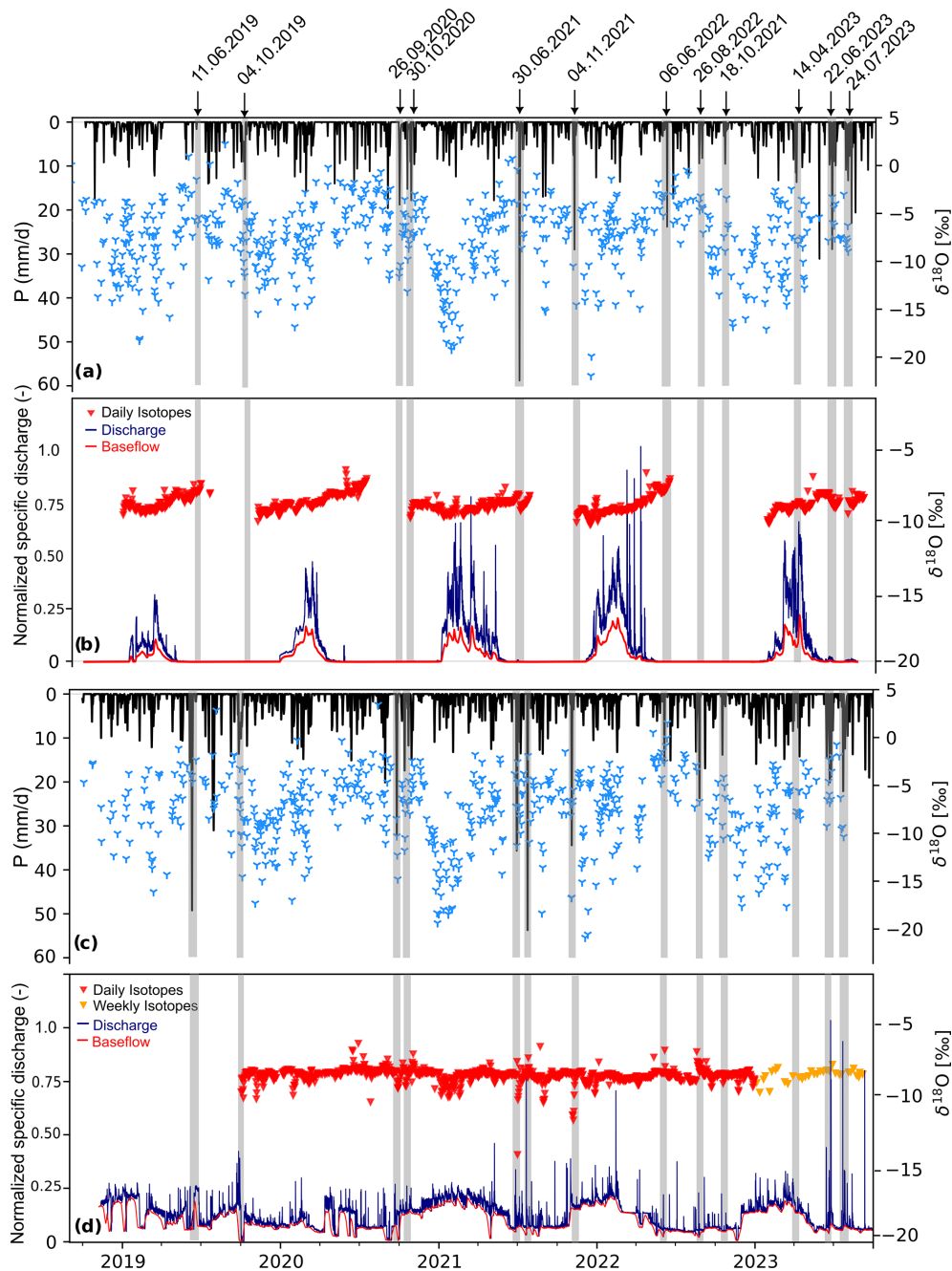
Figure 2. Time series of daily precipitation (black) and precipitation $\delta^{18}O$ isotopes (light blue) in the **(a)** rural and **(c)** urban catchments; time series of hourly discharge (blue) and daily streamflow $\delta^{18}O$ isotopes (red) in the **(b)** rural and **(d)** urban streams. Baseflow is indicated in red as part of the discharge time series. In the urban stream, weekly isotopes (orange) are indicated from 2023 onwards. Gray shading indicates selected storm events.

able they are – meaning that a more constant and similar water source is present in the stream, while points spread larger apart indicate greater seasonal variability in the source water contributions. Occasionally highly enriched signatures can be seen following larger summer convective storms. The differences in catchment characteristics (runoff, climate) and urban water management were reflected in the daily iso-

topic signatures of the streams (Figs. 2, 4). While in the rural stream distinct effects of evaporative fractionation were evident in early summer samples from ponded water in riparian areas and wetlands, as well as near beaver dams after intense storm events (Fig. 4a), the majority of the urban stream samples plotted below the LMWL, indicating evaporation (Fig. 4b). Still, the streamflow signature in the urban
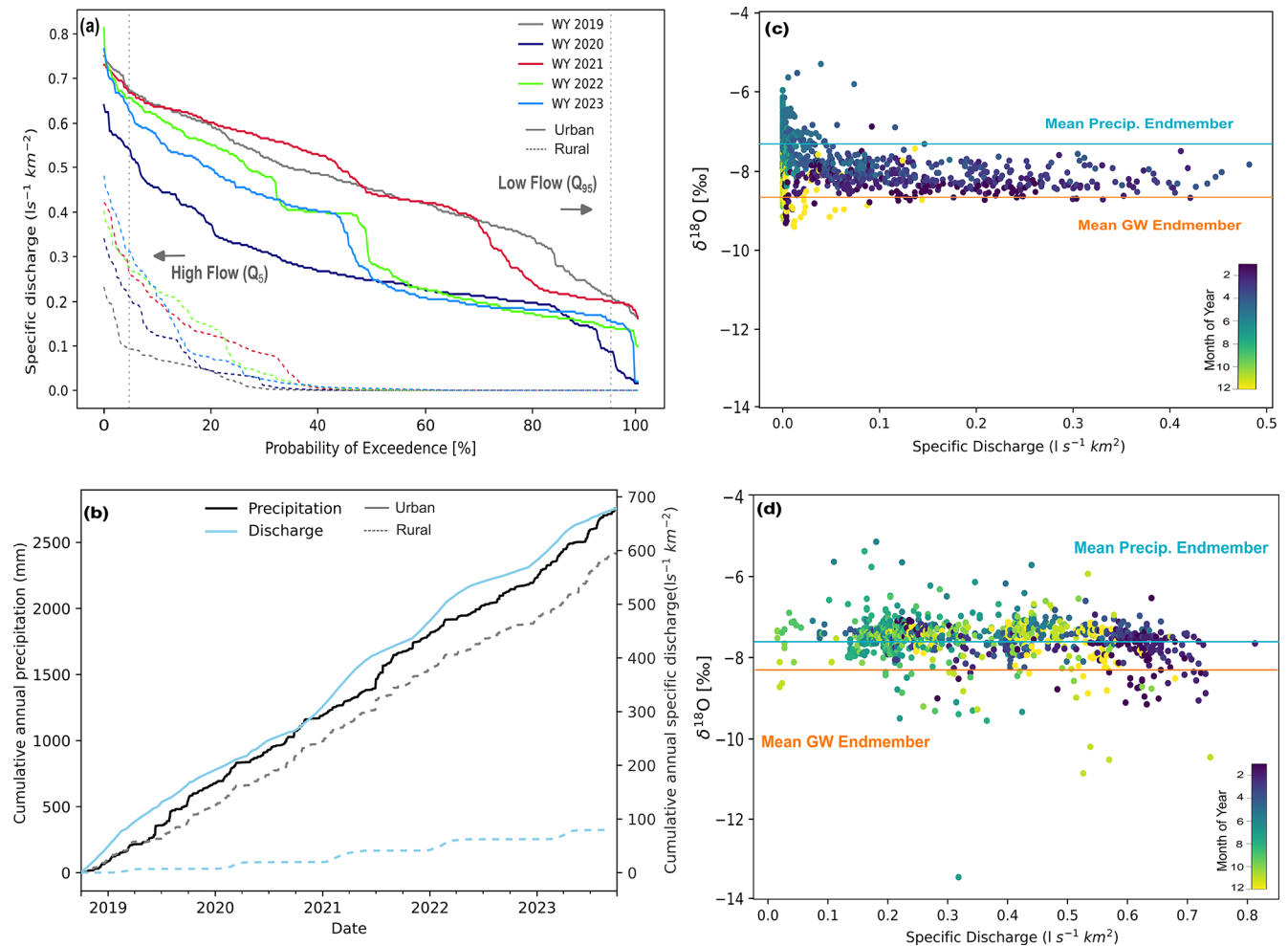
Figure 3. (a) Annual flow duration curves per water year using daily streamflow data for the rural (dotted lines) and urban (solid lines) streams. The stream in the rural catchment shows a characteristic intermittency with much higher likelihood of drying, while the urban catchments are clearly perennial with only ephemeral high flows. **(b)** Double-mass curves of cumulative precipitation and specific discharge over the study period for both streams. **(c, d)** Relationships between daily stream water $\delta^{18}O$ and specific discharge for the rural and urban streams, respectively. Horizontal lines indicated mean measured groundwater (GW; orange) and mean precipitation (blue) endmember $\delta^{18}O$.

stream was more variable and less damped than in the rural stream, indicating occasionally pronounced responses in urban storm drains, which is as important as the limited temporal variability (Fig. 5b).

The most notable seasonal differences were evident in early streamflow samples from the rural stream between December and January (mean $\delta^{18}O = -8.36\,‰$), which resembled groundwater (mean $\delta^{18}O = -8.7\,‰$, SD $= 0.18\,‰$; mean $\delta^2H = -58.9\,‰$, SD $= 0.9\,‰$), while later in the season the influence of recent precipitation was more pronounced (mean $\delta^{18}O = -7.2\,‰$) (Fig. 3a; also see Fig. S2). Lc-excess in the rural stream frequently showed negative values and a strong seasonality ($0.8\,‰$ to $-11\,‰$), a clear sign of the seasonal fractionation from late spring to early summer during and prior to streamflow cessation. Because of the overwhelming influence of effluents, more enriched

signals in the stream could be seen in summer (mean $\delta^{18}O = -7.4\,‰$), which are likely attributable to an increased inflow of enriched effluents. Because the upper urban catchment also receives water from a north-bank tributary which drains forested and wetland areas, the variable inflow of differently fractionated water sources was visible in the lc-excess signal which showed strong variability ($-7.9\,‰$ to $4.3\,‰$). Lower lc-excess values were estimated in winter, reflecting the inflow of more fractionated sources (e.g., wastewater, lake water). Positive lc-excess values were noted only following rain events.

4.4 Inferring stream water age and transit times from isotope data

Estimates of average young water fractions (F_{yw}) (in this case percentage of water younger than 2–3 months) are
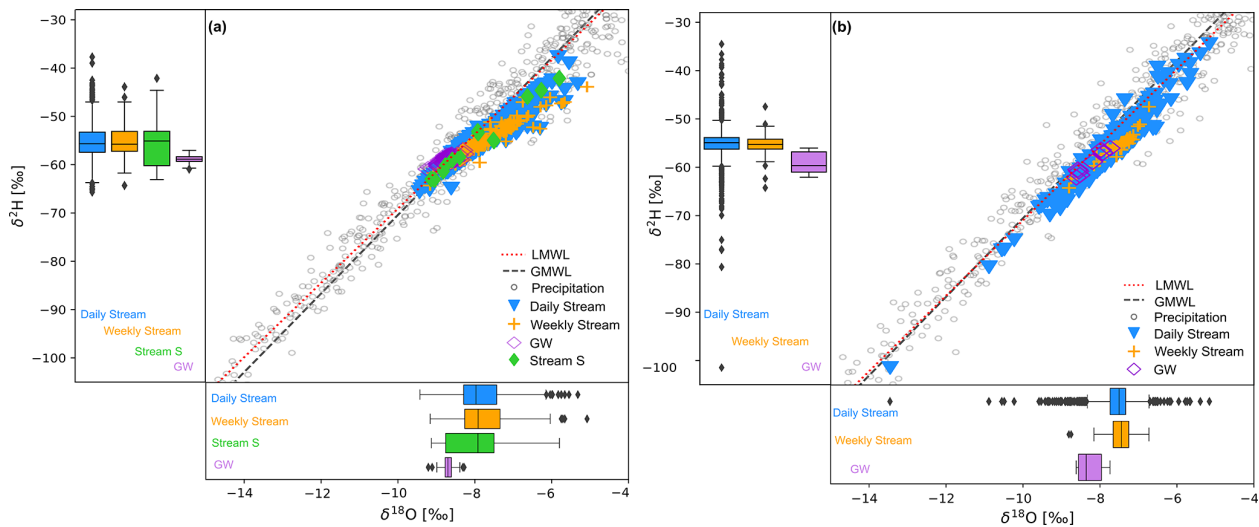
Figure 4. Dual isotope (center) and boxplots (left, bottom) showing the isotopic composition of daily precipitation (gray), daily streamflow (blue), weekly streamflow (orange) and groundwater isotopes (purple) in the **(a)** rural and **(b)** urban catchments. Additional isotope samples (Stream S; green) from isolated pools in the rural stream are shown for the rural catchment. The global meteoric water line (GMWL, black) and amount-weighted local meteoric water lines (LMWL, red) from precipitation signals are shown for reference.
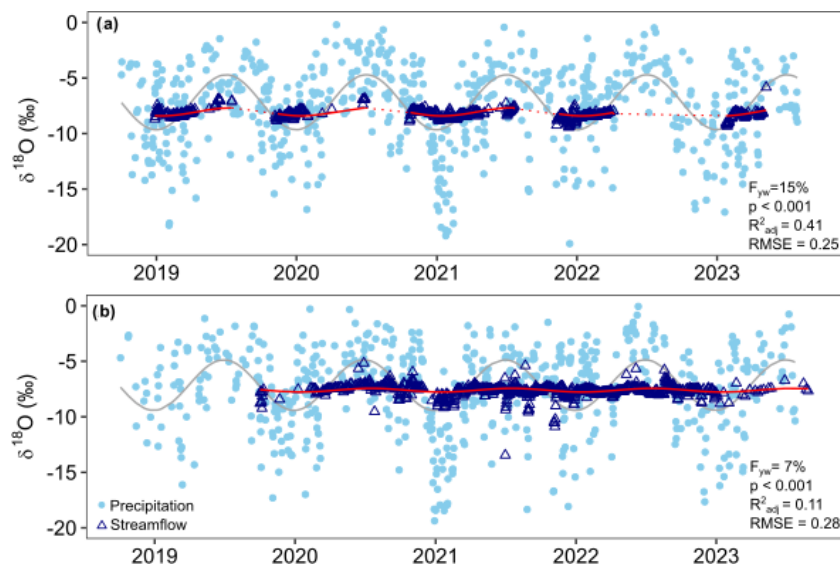
Figure 5. Isotopic seasonality of precipitation (light blue) and streamflow (dark blue) for the **(a)** rural and **(b)** urban streams. Sinusoidal cycles were fitted to precipitation (gray) and daily stream isotope (red) data using iteratively weighted least squares regression (IRLS) (based on von Freyberg et al., 2018) for estimates of young water contributions (F_{YW}) (< 2–3 months). Periods of no flow in the rural catchment are noted with dotted lines in the sinusoidal fitting.

shown in Fig. 5. In the rural catchment, the average young water fraction was $\sim 15\%$ ($p < 0.001$, $R^2_{adj} = 0.41$, RMSE $= 0.25$) (Fig. 5a), while in the urban stream young water estimations were relatively low, averaging around 7% ($p < 2.2 \times 10^{-16}$, $R^2_{adj} = 0.11$, RMSE $= 0.28$), despite the significant amounts of urban storm drainage (Fig. 5b). For individual water years, the model suggests some interannual variability in the rural catchment between wetter and drier years, with young water contributions ranging from ~ 10 up

to $\sim 35\%$, while the generally limited interannual variability in the urban stream, with estimates only between 5% to 15%, was a clear indication of the time-variant contributions of younger water that includes urban water sources (including wastewater discharge and storm drains) as well as precipitation (Table 2). Notably, the different catchment responses to precipitation can be seen in the negative correlation of mean annual young water fractions to annual precipitation ($r = -0.67$, $p < 0.01$) and annual discharge

($r = -0.61$, $p < 0.01$) in the rural catchment, while they were positively correlated with annual precipitation totals ($r = 0.47$, $p < 0.01$) and negatively correlated with annual discharge ($r = -0.49$, $p < 0.01$) in the urban catchment. This is broadly consistent with the greater impact of precipitation events during the winter and spring season, as well as greater urban drainage and fast flowpaths, which are activated in response to intense summer precipitation, as seen in the highest urban F_{yw} ($\sim 15\%$) in 2023 (Table 2).

Most notably for WY 2019, despite low runoff and overall low precipitation in the rural Brandenburg region, F_{yw} was surprisingly high at around 37%, consistent with a low BFI (~ 0.5) (Table 1). At the same time for WY 2023, F_{yw} was also estimated to be around 30%, which would be more consistent with increased contributions of precipitation to streamflow during the wet spring and intense summer convective events. Similarly, the rain-intensive period of early 2023 and subsequent intense summer convective events also resulted in an increased young water contribution of up to 15% in the urban catchment, while F_{yw} values were lowest in WYs 2021 and 2022, with estimates of around 5% also consistent with higher BFI values (~ 0.8) (Table 1).

The TTDs from the TPLR and gamma models were fitted successfully to both streams (Fig. 6; see Table S4 for further model results). The TPLR model gave slightly better fits for modeled $\delta^{18}O$ values than the gamma model in terms of NSE statistics and R^2 (Table 4). Estimated MTTs were distinctly higher for the TPLR, ranging between 3 and 4 years for the rural and urban streams, respectively, while MTTs with the gamma model were only estimated to be less than 2 years for both streams. The median fast and slow transit times (τ_f and τ_s) were 22 and 1262 d for the rural stream and 5 and 1311 d for the urban stream. Despite inherent limitations in the detectability of stream water $\delta^{18}O$ signatures older than 5 years, the TPLR model was useful in capturing the rapidly responding flowpaths through the fast component, which drives streamflow flashiness in both streams. The fast-flow contributions were also similar to the range of F_{yw} estimates (rural: $\tau_f \sim 22$ d, $F_{yw} \sim 15\%$; urban: $\tau_f \sim 5$ d, $F_{yw} \sim 7\%$). Nevertheless, especially in the rural stream, both models fail to capture the streamflow signatures towards summer, especially during the 2019 period, but appear to work well for the wet periods of 2023. Furthermore, in early 2021, the influence of the more depleted winter precipitation on streamflow was overestimated. The more damped isotopic dynamics of the urban stream were generally well captured in both models, with only the most short-term responses to the severely depleted high-intensity convectional events (i.e., summer 2021) and the occasional inflow of more enriched sources (e.g., effluents) not being fully captured.

5 Discussion

5.1 Seasonal and event flow responses

Recent severe drought hazards across central Europe have highlighted the vulnerability of streams to the compound effects of drought on frequency of intermittency and longevity of zero-flow periods (Creutzfeldt et al., 2021; Sarremejane et al., 2022; Tramblay et al., 2021). In Berlin–Brandenburg, the 2018 drought and sustained negative rainfall anomalies in subsequent years exacerbated a decade-long trend of declining groundwater levels, causing increasing disconnectivity between groundwater and surface water and raising concerns regarding future water availability, especially in less-managed agricultural areas but also in cities like Berlin (Creutzfeldt et al., 2021; DWD, 2019). Propagation of precipitation deficits into groundwater droughts is particularly detrimental in areas where groundwater is the main contributor to baseflow, as in the case of the rural stream (up to 70%) but also in cities where groundwater and bank filtration are the main sources of water supply, as is the case in Berlin. Consequently, flow regimes in similar drought-sensitive lowland areas are exposed to hydroclimate hazards and land use change impacts (Luo et al., 2024; Paredes del Puerto et al., 2024; Van Loon and Laaha, 2015; Wunsch et al., 2022).

Compared to the long-term mean discharge of the rural catchment ($0.11\,m^3\,s^{-1}$, 2001–2017; Ying et al., 2024), daily discharge has declined by up to 60% following the 2018 drought. Due to the limited replenishment of moisture during winter in 2018–2019, the observed low discharge and longer no-flow periods defined 2018–2019 and the subsequent hydrological years. The lack of summer streamflow response to even the largest precipitation events (e.g., June 2021) coincided with observed soil moisture deficits as well as limited groundwater recharge, resulting in limited surface water connectivity and streamflow generation (Landgraf et al., 2022; Ying et al., 2024). This also affected nutrient transport and chemodynamic behavior, as low flows decreased transport capacity and dilution effects (Wu et al., 2021).

Through daily isotopic signatures, the close link to seasonal groundwater and the relative elasticity in the streamflow response to the timing of precipitation became evident (for more detail see Figs. S2 and S3). The importance of seasonal precipitation in maintaining streamflow connectivity and the groundwater for generating winter streamflow generation could be confirmed through the seasonal isotopic signal. Nevertheless, increasing ET and projected precipitation decreases may compromise the catchments' ability to maintain green and blue water fluxes throughout the year in areas with lower water retention. Especially in agricultural catchments, the dominance of green water fluxes from water-intensive crops such as maize and other cereals can propagate inter-year drought memory effects from reduced blue water fluxes to groundwater recharge and streamflow generation (Ihinegbu and Ogunwumi, 2022; Orth and Seneviratne,
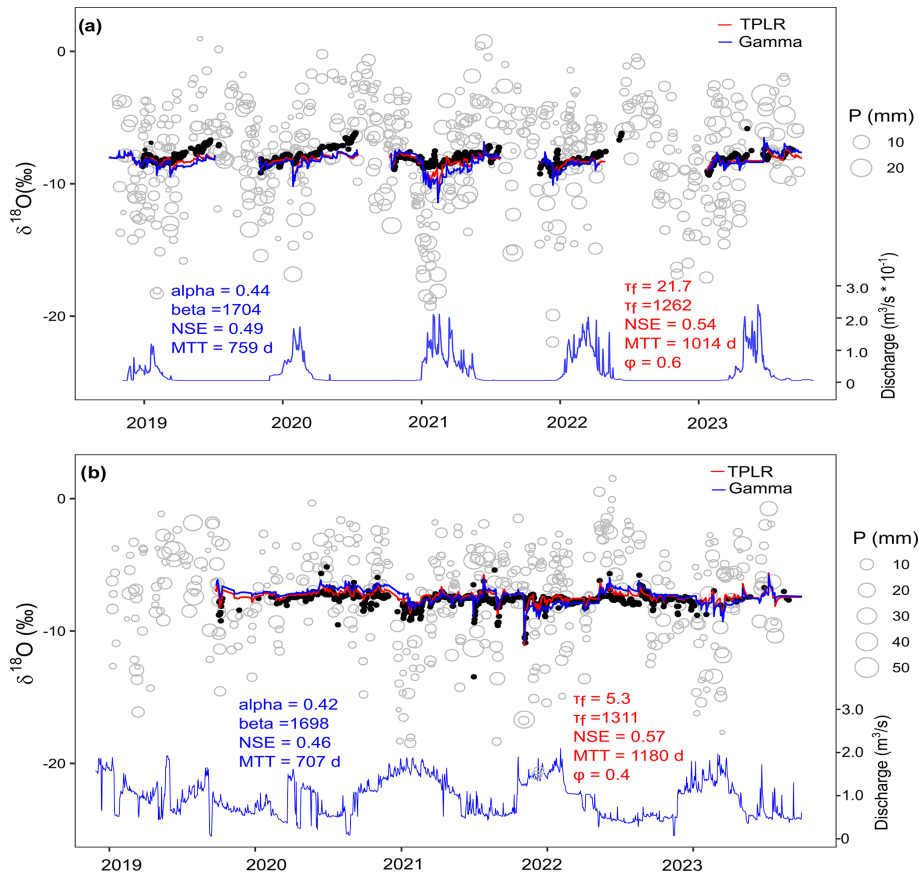
Figure 6. Fitted transit time distributions expressed as cumulative distribution functions using the two-parallel linear reservoir (TPLR) model (red) and gamma model (blue) for the **(a)** rural and **(b)** urban catchments. Precipitation amount (in mm) is denoted by the size of the open circles, and isotopic values of precipitation inputs correspond with the y axis (‰) on the left. Periods of no flow in the rural catchment have been indicated with a gap in the simulations. Daily discharge is shown in blue ($m^3\,s^{-1}$).

2013), creating uncertainty over the resilience of agricultural production and land use (Beillouin et al., 2020; McNamara et al., 2024)

The contrasting urban streamflow responses to drought and seasonal precipitation illustrated not only the effects of urban water management, but also the impacts of progressive urbanization and land use changes on streamflow dynamics. While baseflow in the urban stream was only slightly lower during drier years, overall discharge was defined by the increased discharge of wastewater treatment plant (WWTP) effluents, which can regularly account for up to 90 % of total discharge (Marx et al., 2021). The moderated drought response of streamflow in WYs 2019 and 2020 underscored the crucial role of effluents in sustaining baseflows during extreme drought periods (Luthy et al., 2015) and the impact of baseflow regulation and runoff following storm events. The influence of urban water management on rapid flowpaths, interbasin water transfers and streamflow generation defines many urban systems, with urban groundwater recharge and baseflow being shaped by urban infrastructure and development (Bhaskar et al., 2016). At the same time natural hazards

such as floods and droughts increasingly challenge not only water availability resilience, but also managers' ability to tailor resource management approaches to changes in local climate conditions (Hale et al., 2016). The broader interaction of the urban stream network with the surrounding environment and the different urban water sources (i.e., wetlands, floodplains, built environment) clearly shape the downstream propagation of a flood peak through the urban catchment (Johnson et al., 2022; Oswald et al., 2023). In times of increased drought and flood hazards, urban catchment responses to natural hazards need to be strengthened even more by preserving and enhancing wetland areas in peri-urban and rural areas and by allowing the infiltration and storage of excess surface water through nature-based solutions (Davis and Naumann, 2017; Green et al., 2021).

5.2 Transit times and water ages

Estimates of young water fractions, MTTs and TTDs provided a rough approximation of complex age and transit time distributions due to limitations of the F_{yw} approach

(Kirchner, 2016; Seeger and Weiler, 2014) and the inability of lumped convolution models to account for evaporative fractionation and mixed water sources (McGuire and McDonnell, 2006). The relatively low young water fractions of $\sim 7\%$ in the urban stream, despite significant urban runoff, further highlight the complicating issue of constraining water ages in urban streams, where an overwhelming dominance of mixed urban sources weakens the influence and differentiation of recent precipitation (Bonneau et al., 2018; Soulsby et al., 2014). This is a particular impediment in closed urban water management systems, such as Berlin, where there is overlap in the isotopic composition of surface water, groundwater and wastewater contributions (Massman et al., 2008).

In the rural catchment, the longer, continuous time series of daily stream and precipitation isotopes over 5 years allowed for a more systematic filtering of fractionated signals of early summer streamflow, as previous estimates from only < 2 years of daily data indicated high levels of uncertainty in MTT and F_{yw} estimates (Kleine et al., 2021). Our results not only revealed interannual differences in young water contributions related to annual precipitation, but also improved young water fraction estimates for different years with lower values between 0.1 and 0.37 (mean 0.15) compared to previous estimates (mean 0.37; Kleine et al., 2021). These values are more consistent with estimates from other lowland catchments in central Germany (Lutz et al., 2018) and only slightly below the median young water fraction of 26% for European catchments (Jasechko et al., 2016). The larger F_{yw} in the rural stream compared to the urban may be attributed to the smaller catchment size, whereby the predominantly agricultural land use (drainage and compaction) likely facilitates rapid runoff responses via the artificial drainage pipes and channels, thus driving the release of young water contributions to the stream from relatively small areas in the catchment (Von Freyberg et al., 2018; Lutz et al., 2018). However, the higher F_{yw} in the rural stream during the drought may well also be an artifact of the method, as the data collection period was also limited due to the stream's intermittency. Fractionation effects or difficulties in constraining water sources invariably increase the uncertainties associated with the non-stationarity of TTDs over different timescales in response to hydroclimatic conditions (Hrachowitz et al., 2010). As a result, particularly during the drought this may produce a less-robust seasonal cycle coefficient for each individual hydrological period, as evidenced by the overall higher uncertainty attached to F_{yw} estimates in drier years (Table 2).

Regarding TTDs and estimated MTTs, our estimates for the rural catchment between 2–4 years (730–1622 d), with the higher estimate from the TPLR model, are considered more likely and within the range of tritium estimates of water age of local groundwater of around 5 years (Ying et al., 2024) and stream water ages of ~ 7 years (Smith et al., 2021). Still, similar to previously noted limitations in MTT estimations in such lowland areas (Tetzlaff et al., 2011), the perva-

sive influence of older groundwater in the rural stream likely weakens the influence of precipitation intensity on MTTs, as evidenced by the occasional overprediction of isotopic response in the stream during early flow periods in winter (e.g., early 2021) (Fig. 6a). The better performance of the TPLR compared to the gamma model in the urban catchment underlines the particular suitability of the two-reservoir model in an urban environment, where runoff generation follows a more binary distribution (Soulsby et al., 2014). Nevertheless, a caveat to these conclusions is again the extreme damping of isotope signatures in the urban stream due to the overwhelming influence of effluents, which limits the ability of both models to constrain the hydro-demographics of different water sources (e.g., groundwater, precipitation) in a conclusive manner (Sprenger et al., 2019)

5.3 Wider implications

With the projected changes for Europe suggesting a greater seasonal divergence of lower and higher precipitation amounts in summer and winter, respectively, the seasonal synchronicity of groundwater baseflow responses we found in our study may widen even further, as the longer timescales for groundwater recovery after extended precipitation deficits usually lags behind by several years despite the return to wetter conditions (Hellwig et al., 2020; Smith et al., 2022). The effects of such hydroclimate changes may be even more severe in urban areas, where urbanization has directly been linked with the intensification of extreme rainfall (Singh et al., 2020). Urban "plumbing", a high level of imperviousness and lack of urban green space can reduce recharge and groundwater storage to the point where they are unable to buffer natural climate variability, requiring even more extensive water management (Bonneau et al., 2018; Marx et al., 2021; Oswald et al., 2023). As such, the main novelty of this paper stems from the long time series of isotopes, as it gives context to understanding different catchment responses.

The differential impacts of drought and extreme events on streamflow generation are conceptualized in Fig. 7, illustrating different seasonal controls on flow permanence and magnitude of associated hydrological processes in contrasting environments. During drought periods with reduced rainfall and high ET, severe soil moisture deficits and low recharge increase the disconnection between surface and groundwater, leading to long-lasting groundwater droughts, reduced agricultural production and increased streamflow intermittency. Conversely, extensive water management can moderate drought impacts through the supply of wastewater effluents or other continuous sources, but this in turn can lead to increased nutrient concentration and negative impacts on freshwater quality and microbial diversity (Numberger et al., 2022; Warter et al., 2024). In the context of natural hazards and climate change, more frequent and intense rain events and flooding can challenge urban infrastructure and inner-city drainage systems, as greater quantities of water also in-
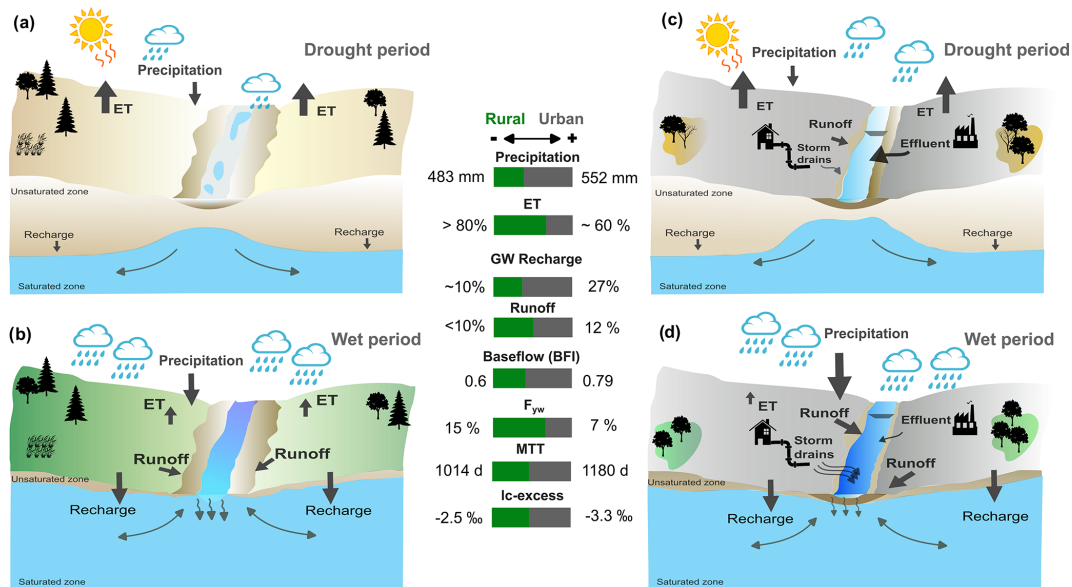
Figure 7. Conceptual summary of dynamics in hydrological processes and metrics in the rural agricultural and urban catchments during **(a, c)** drought periods and **(b, d)** wet periods. Bars in the middle represent the general magnitude of fluxes in each catchment in comparison.

crease organic pollutant loads and threaten aquatic habitats and biodiversity (Creutzfeldt et al., 2021; Haase et al., 2023).

Nevertheless, there is a need to reconcile different water use requirements and management approaches that preserve the hydrological and ecological integrity, which is inherently more difficult with insufficient information on hydrological process dynamics and land use influences. Especially in urban systems, which encompass engineered management systems as well as natural systems, a conjoint understanding of basic hydrologic processes is urgently needed (Gessner et al., 2014). Emerging questions of whether declining baseflows should be seasonally augmented by treated wastewater or interbasin water transfer not only are a matter of social choice but also require consideration of the hydrological, ecological and chemical impacts of increased baseflow contributions on instream habitat, biodiversity targets and water quality (Numberger et al., 2022; Warter et al., 2024). Designing flow regimes to achieve specific ecological and hydrological restoration goals may become the norm in modified and managed rivers where a return to natural, pre-anthropic conditions is no longer feasible and a maintenance of certain flow levels is governed by different targets (Acreman et al., 2014; Stewardson et al., 2017). As such, identifying thresholds at which important hydrological changes occur requires a thorough understanding of how water moves through catchment systems, for which tracer studies are an invaluable tool to understand water resource systems and their vulnerability to hydroclimate changes (Ehleringer et al., 2016).

6 Conclusion

Intercatchment comparisons between urban and rural stream systems using multiyear tracer-based assessments are still rare but are – as demonstrated here – very insightful and much needed. From the strong responses to drought and an increasing hydroclimatic variability, land use (i.e., drainage, vegetation, wetland restoration) was shown to be important in water partitioning of groundwater–surface-water interactions and streamflow generation in these anthropogenically impacted streams. Our results not only highlighted the continued importance and value of high-resolution long-term tracer data to develop a synoptic understanding of the principal hydrologic mechanisms by which flow regimes directly and indirectly respond to climate perturbations, especially in understudied urban environments, but also provided immediate evidence of contrasting catchment functioning and streamflow generation in different geographical settings, which will be useful for the identification of future environmental flow assessments in similar urban and lowland catchments where a return to pre-anthropic natural conditions may no longer be attainable. The limitations in the detection of water ages and source contributions in the urban stream highlighted the need for long-term tracer-based assessments of urban hydrological fluxes, using either stable isotopes or other reactive tracers, to better constrain current and future inter- and intra-annual variability and to mitigate the effects of hazards such as floods and droughts. Although the challenges associated with sustained monitoring often limit long-term observations over broader scales, the benefits and value of long-term observations are crucial for hydrologists, ecologists, urban planners and local stakeholders

interested in protecting and maintaining ecosystem functions and managing future water resources in the most sustainable and integrated way that reduces environmental impacts and economic costs.

Supplement. The supplement related to this article is available online at: https://doi.org/10.5194/nhess-24-3907-2024-supplement.

Author contributions. Conceptualization: DT, CS, MMW. Methodology: MMW, CM, DT, CS. Investigation: CM, MMW. Formal analysis: MMW. Data curation: MMW, CM. Writing (original draft): MMW. Writing (review and editing): DT, CS. Visualization: MMW. Supervision: DT, CS. Funding acquisition: DT, CS.

Competing interests. The contact author has declared that none of the authors has any competing interests.

Disclaimer. Publisher's note: Copernicus Publications remains neutral with regard to jurisdictional claims made in the text, published maps, institutional affiliations, or any other geographical representation in this paper. While Copernicus Publications makes every effort to include appropriate place names, the final responsibility lies with the authors.

Special issue statement. This article is part of the special issue "Current and future water-related risks in the Berlin–Brandenburg region". It is not associated with a conference.

Review statement. This paper was edited by Márk Somogyvári and reviewed by two anonymous referees.

References

Acreman, M., Arthington, A. H., Colloff, M. J., Couch, C., Crossman, N. D., Dyer, F., Overton, I., Pollino, C. A., Stewardson, M. J., and Young, W.: Environmental flows for natural, hybrid, and novel riverine ecosystems in a changing world, Front. Ecol. Environ., 12, 466–473, https://doi.org/10.1890/130134, 2014.

Arthington, A. H., Bunn, S. E., Poff, N. L. R., and Naiman, R. J.: The challenge of providing environmental flow rules to sustain river ecosystems, Ecol. Appl., 16, 1311–1318, https://doi.org/10.1890/1051-0761(2006)016[1311:TCOPEF]2.0.CO;2, 2006.

Baker, D. B., Richards, R. P., Loftus, T. T., and Kramer, J. W.: A new flashiness index: Characteristics and applications to Midwestern rivers and streams, J. Am. Water Resour. As., 40, 503–522, https://doi.org/10.1111/j.1752-1688.2004.tb01046.x, 2004.

Beillouin, D., Schauberger, B., Bastos, A., Ciais, P., and Makowski, D.: Impact of extreme weather conditions on European crop production in 2018: Random forest – Yield anomalies, Philos. T. R. Soc. B, 375, 20190510, https://doi.org/10.1098/rstb.2019.0510, 2020.

Bhaskar, A. S., Beesley, L., Burns, M. J., Fletcher, T. D., Hamel, P., Oldham, C. E., and Roy, A. H.: Will it rise or will it fall? Managing the complex effects of urbanization on base flow, Freshw. Sci., 35, 293–310, https://doi.org/10.1086/685084, 2016.

Birkel, C., Geris, J., Molina, M. J., Mendez, C., Arce, R., Dick, J., Tetzlaff, D., and Soulsby, C.: Hydroclimatic controls on non-stationary stream water ages in humid tropical catchments, J. Hydrol., 542, 231–240, https://doi.org/10.1016/j.jhydrol.2016.09.006, 2016.

Bonneau, J., Burns, M. J., Fletcher, T. D., Witt, R., Drysdale, R. N., and Costelloe, J. F.: The impact of urbanization on subsurface flow paths – A paired-catchment isotopic study, J. Hydrol., 561, 413–426, https://doi.org/10.1016/j.jhydrol.2018.04.022, 2018.

Creutzfeldt, B., Pohle, I., Zeilfelder, S., Birner, J., Köhler, A., Von Seggern, D., and Rehfeld-Klein, M.: Die Niedrigwasserjahre 2018, 2019 und 2020 – Analysen und Auswirkungen für das Land Berlin, Berlin, https://www.berlin.de/sen/uvk/umwelt/wasser-und-geologie/niedrigwasser/ (last access: 9 January 2024), 2021.

Davis, M. and Naumann, S.: Making the Case for Sustainable Urban Drainage Systems as a Nature-Based Solution to Urban Flooding, 123–137, https://doi.org/10.1007/978-3-319-56091-5_8, 2017.

Döll, P. and Schmied, H. M.: How is the impact of climate change on river flow regimes related to the impact on mean annual runoff? A global-scale analysis, Environ. Res. Lett., 7, 014037, https://doi.org/10.1088/1748-9326/7/1/014037, 2012.

DWD: Klimareport Brandenburg, 1. Auflage, Deutscher Wetterdienst, Offenbach am Main, Deutschland, 40

pp., https://www.dwd.de/DE/leistungen/klimareport_bb/klimareport_bb_2019_download.pdf:jsessionid=B395D9FED0D8CDF3CD59C5868097F952.live11041?__blob=publicationFile&v=5, (last access: 13 December 2023), 2019.

DWD: Index of /climate_environment/CDC/, DWD [data set], https://opendata.dwd.de/climate_environment/CDC/ (last access: 18 December 2023), 2023.

Ehleringer, J. R., Barnette, J. E., Jameel, Y., Tipple, B. J., Bowen, J., Ehleringer, J. R., Barnette, J. E., Jameel, Y., and Tipple, B. J.: Urban water – a new frontier in isotope hydrology, Isot. Environ. Healt. S, 52, 477–486, https://doi.org/10.1080/10256016.2016.1171217, 2016.

Gessner, M. O., Hinkelmann, R., Nützmann, G., Jekel, M., Singer, G., Lewandowski, J., Nehls, T., and Barjenbruch, M.: Urban water interfaces, J. Hydrol., 514, 226–232, https://doi.org/10.1016/j.jhydrol.2014.04.021, 2014.

Green, D., Donnell, E. O., Slater, L., Chan, F. K. S., Thorne, C., Li, L., Boothroyd, R. J., and Stirling, R.: Green infrastructure: The future of urban flood risk management?, WIREs Water, 8, e1560, https://doi.org/10.1002/wat2.1560, 2021.

Haase, P., Bowler, D. E., Baker, N. J., Bonada, N., Domisch, S., Garcia Marquez, J. R., Heino, J., Hering, D., Jähnig, S. C., Schmidt-Kloiber, A., Stubbington, R., Altermatt, F., Álvarez-Cabria, M., Amatulli, G., Angeler, D. G., Archambaud-Suard, G., Jorrín, I. A., Aspin, T., Azpiroz, I., Bañares, I., Ortiz, J. B., Bodin, C. L., Bonacina, L., Bottarin, R., Cañedo-Argüelles, M., Csabai, Z., Datry, T., de Eyto, E., Dohet, A., Dörflinger, G., Drohan, E., Eikland, K. A., England, J., Eriksen, T. E., Evtimova, V., Feio, M. J., Ferréol, M., Floury, M., Forcellini, M., Forio, M. A. E., Fornaroli, R., Friberg, N., Fruget, J.-F., Georgieva, G., Goethals, P., Graça, M. A. S., Graf, W., House, A., Huttunen, K.-L., Jensen, T. C., Johnson, R. K., Jones, J. I., Kiesel, J., Kuglerová, L., Larrañaga, A., Leitner, P., L'Hoste, L., Lizée, M.-H., Lorenz, A. W., Maire, A., Arnaiz, J. A. M., McKie, B. G., Millán, A., Monteith, D., Muotka, T., Murphy, J. F., Ozolins, D., Paavola, R., Paril, P., Peñas, F. J., Pilotto, F., Polášek, M., Rasmussen, J. J., Rubio, M., Sánchez-Fernández, D., Sandin, L., Schäfer, R. B., Scotti, A., Shen, L. Q., Skuja, A., Stoll, S., Straka, M., Timm, H., Tyufekchieva, V. G., Tziortzis, I., Uzunov, Y., van der Lee, G. H., Vannevel, R., Varadinova, E., Várbíró, G., Velle, G., Verdonschot, P. F. M., Verdonschot, R. C. M., Vidinova, Y., Wiberg-Larsen, P., and Welti, E. A. R.: The recovery of European freshwater biodiversity has come to a halt, Nature, 620, 582–588, https://doi.org/10.1038/s41586-023-06400-1, 2023.

Hale, R. L., Scoggins, M., Smucker, N. J., and Suchy, A.: Effects of climate on the expression of the urban stream syndrome, Freshw. Sci., 35, 421–428, https://doi.org/10.1086/684594, 2016.

Hellwig, J., de Graaf, I. E. M., Weiler, M., and Stahl, K.: Large-Scale Assessment of Delayed Groundwater Responses to Drought, Water Resour. Res., 56, e2019WR025441, https://doi.org/10.1029/2019WR025441, 2020.

Hrachowitz, M., Soulsby, C., Tetzlaff, D., Malcolm, I. A., and Schoups, G.: Gamma distribution models for transit time estimation in catchments: Physical interpretation of parameters and implications for time-variant transit time assessment, Water Resour. Res., 46, W10536, https://doi.org/10.1029/2010WR009148, 2010.

Ihinegbu, C. and Ogunwumi, T.: Multi-criteria modelling of drought: a study of Brandenburg Federal State, Germany, Model. Earth Syst. Environ., 8, 2035–2049, https://doi.org/10.1007/s40808-021-01197-2, 2022.

Jasechko, S.: Global Isotope Hydrogeology – Review, Rev. Geophys., 57, 835–965, https://doi.org/10.1029/2018RG000627, 2019.

Jasechko, S., Kirchner, J. W., Welker, J. M., and McDonnell, J. J.: Substantial proportion of global streamflow less than three months old, Nat. Geosci., 9, 126–129, https://doi.org/10.1038/ngeo2636, 2016.

Johnson, B. G., Morris, C. S., Mase, H. L., Whitehouse, P. S., and Paradise, C. J.: Seasonal flashiness and high frequency discharge events in headwater streams in the North Carolina Piedmont (United States), Hydrol. Process., 36, 1–19, https://doi.org/10.1002/hyp.14550, 2022.

Kendall, C. and McDonnell, J. J.: Isotope Tracers in Catchment Hydrology, Elsevier, Amsterdam, ISBN 978-0-444-501555-X, 1998.

Kirchner, J. W.: Aggregation in environmental systems – Part 1: Seasonal tracer cycles quantify young water fractions, but not mean transit times, in spatially heterogeneous catchments, Hydrol. Earth Syst. Sci., 20, 279–297, https://doi.org/10.5194/hess-20-279-2016, 2016.

Kleine, L., Tetzlaff, D., Smith, A., Wang, H., and Soulsby, C.: Using water stable isotopes to understand evaporation, moisture stress, and re-wetting in catchment forest and grassland soils of the summer drought of 2018, Hydrol. Earth Syst. Sci., 24, 3737–3752, https://doi.org/10.5194/hess-24-3737-2020, 2020.

Kleine, L., Tetzlaff, D., Smith, A., Dubbert, M., and Soulsby, C.: Modelling ecohydrological feedbacks in forest and grassland plots under a prolonged drought anomaly in Central Europe 2018–2020, Hydrol. Process., 35, 1–20, https://doi.org/10.1002/hyp.14325, 2021a.

Kleine, L., Smith, A., and Goldhammer, T.: Using isotopes to understand landscape-scale connectivity in a groundwater-dominated, lowland catchment under drought conditions, Hydrol. Process., 35, e14197, https://doi.org/10.1002/hyp.14197, 2021b.

Kuhlemann, L. M., Tetzlaff, D., and Soulsby, C.: Urban water systems under climate stress: An isotopic perspective from Berlin, Germany, Hydrol. Process., 34, 3758–3776, https://doi.org/10.1002/hyp.13850, 2020.

Landesvermessung und Geobasisinformation Brandenburg (LGB), ALKIS-Daten – ProduktmetadatenjGeobroker – Der Internetshop der LGB. Geobroker, https://geobroker.geobasis-bb.de/gbss.php?MODE=GetProductInformation&PRODUCTID=6de36219-3e68-489e-8ebc-632e5ffb6dc9 (last access: 12 September 2023), 2020.

Landgraf, J., Tetzlaff, D., Freymüller, J., and Soulsby, C.: Using stable water isotopes to understand ecohydrological partitioning under contrasting land uses in a drought-sensitive rural, lowland catchment, Hydrol. Process., 36, e14779, https://doi.org/10.1002/hyp.14779, 2022.

Landwehr, J. M. and Coplen, T.: Line-conditioned excess: a new method for characterizing stable hydrogen and oxygen isotope ratios in hydrologic systems (IAEA-CN-118/56), in: Isotopes in Environmental Studies, IAEA, Vienna, 132–135, ISBN 92-0-111305-X, 2006.

Nat. Hazards Earth Syst. Sci., 24, 3907–3924, 2024

https://doi.org/10.5194/nhess-24-3907-2024

Lobanova, A., Liersch, S., Nunes, J. P., Didovets, I., Stagl, J., Huang, S., Koch, H., Rivas López, M. del R., Maule, C. F., Hattermann, F., and Krysanova, V.: Hydrological impacts of moderate and high-end climate change across European river basins, J. Hydrol. Reg. Stud., 18, 15–30, https://doi.org/10.1016/j.ejrh.2018.05.003, 2018.

Luo, S., Tetzlaff, D., Smith, A., and Soulsby, C.: Assessing impacts of alternative land use strategies on water partitioning, storage and ages in drought-sensitive lowland catchments using tracer-aided ecohydrological modelling, Hydrol. Process., 38, e15126, https://doi.org/10.1002/hyp.15126, 2024.

Luthy, R. G., Sedlak, D. L., Plumlee, M. H., Austin, D., and Resh, V. H.: Wastewater-effluent-dominated streams as ecosystem-management tools in a drier climate, Front. Ecol. Environ., 13, 477–485, https://doi.org/10.1890/150038, 2015.

Lutz, S. R., Krieg, R., Müller, C., Zink, M., Knöller, K., Samaniego, L., and Merz, R.: Spatial Patterns of Water Age: Using Young Water Fractions to Improve the Characterization of Transit Times in Contrasting Catchments, Water Resour. Res., 54, 4767–4784, https://doi.org/10.1029/2017WR022216, 2018.

Marx, C., Tetzlaff, D., Hinkelmann, R., and Soulsby, C.: Isotope hydrology and water sources in a heavily urbanized stream, Hydrol. Process., 35, e14377, https://doi.org/10.1002/hyp.14377, 2021.

Marx, C., Tetzlaff, D., Hinkelmann, R., and Soulsby, C.: Effects of 66 years of water management and hydroclimatic change on the urban hydrology and water quality of the Panke catchment, Berlin, Germany, Sci. Total Environ., 900, 165764, https://doi.org/10.1016/j.scitotenv.2023.165764, 2023.

Massman, G., Sültenfuß, J., Dünnbier, U., Knappe, A., Taute, T., and Pekdeger, A.: Investigation of groundwater residence times during bank filtration in Berlin: a multi-tracer approach, Hydrol. Process., 22, 788–801, https://doi.org/10.1002/hyp.6649, 2008.

McGuire, K. J. and McDonnell, J. J.: A review and evaluation of catchment transit time modeling, J. Hydrol., 330, 543–563, https://doi.org/10.1016/j.jhydrol.2006.04.020, 2006.

McNamara, I., Flörke, M., Uschan, T., Baez-Villanueva, O. M., and Herrmann, F.: Estimates of irrigation requirements throughout Germany under varying climatic conditions, Agr. Water Manage., 291, 108641, https://doi.org/10.1016/j.agwat.2023.108641, 2024.

Nash, J. E. and Sutcliffe, J. V: River flow forecasting through conceptual models part I – A discussion of principles, J. Hydrol., 10, 282–290, https://doi.org/10.1016/0022-1694(70)90255-6, 1970.

Nathan, R. J. and McMahon, T. A.: Evaluation of automated techniques for base flow and recession analyses, Water Resour. Res., 26, 1465–1473, https://doi.org/10.1029/WR026i007p01465, 1990.

Numberger, D., Zoccarato, L., Woodhouse, J., Ganzert, L., Sauer, S., Márquez, J. R. G., Domisch, S., Grossart, H. P., and Greenwood, A. D.: Urbanization promotes specific bacteria in freshwater microbiomes including potential pathogens, Sci. Total Environ., 845, 157321, https://doi.org/10.1016/j.scitotenv.2022.157321, 2022.

O'Briain, R.: Climate change and European rivers: An ecohydromorphological perspective, Ecohydrology, 12, e2099, https://doi.org/10.1002/eco.2099, 2019.

Olden, J. D. and Poff, N. L.: Redundancy and the choice of hydrologic indices for characterizing streamflow regimes, River Res. Appl., 19, 101–121, https://doi.org/10.1002/rra.700, 2003.

Orth, R. and Seneviratne, S. I.: Propagation of soil moisture memory to streamflow and evapotranspiration in Europe, Hydrol. Earth Syst. Sci., 17, 3895–3911, https://doi.org/10.5194/hess-17-3895-2013, 2013.

Oswald, C. J., Kelleher, C., Ledford, S. H., Hopkins, K. G., Sytsma, A., Tetzlaff, D., Toran, L., and Voter, C.: Integrating urban water fluxes and moving beyond impervious surface cover: A review, J. Hydrol., 618, 129188, https://doi.org/10.1016/j.jhydrol.2023.129188, 2023.

Paredes del Puerto, J. M., Sathicq, M. B., Altieri, P., Nicolosi Gelis, M. M., Paracampo, A., Pazos, R. S., Tarda, A. S., Gómez, N., and Colautti, D.: Extreme drought conditions interact with urbanisation, affecting hydrological regimes and water quality in temperate lowland streams, Aquat. Sci., 86, 13, https://doi.org/10.1007/s00027-023-01031-0, 2024.

Paton, E., Vogel, J., Kluge, B., and Nehls, T.: Ausmaß, Trend und Extreme von Dürren im urbanen Raum, Hydrol. Wasserbewirts., HW 65.2021, H.1, https://doi.org/10.5675/HyWa_2021.1_1, 2021.

Poff, N. L. and Zimmerman, J. K. H.: Ecological responses to altered flow regimes: A literature review to inform the science and management of environmental flows, Freshw. Biol., 55, 194–205, https://doi.org/10.1111/j.1365-2427.2009.02272.x, 2010.

Poff, N. L., Allan, J. D., Bain, M. B., Karr, J. R., Prestegaard, K. L., Richter, B. D., Sparks, R. E., and Stromberg, J. C.: The Natural Flow Regime, Bioscience, 47, 769–784, https://doi.org/10.2307/1313099, 1997.

Sarremejane, R., Messager, M. L., and Datry, T.: Drought in intermittent river and ephemeral stream networks, Ecohydrology, 15, e2390, https://doi.org/10.1002/eco.2390, 2022.

Seeger, S. and Weiler, M.: Reevaluation of transit time distributions, mean transit times and their relation to catchment topography, Hydrol. Earth Syst. Sci., 18, 4751–4771, https://doi.org/10.5194/hess-18-4751-2014, 2014.

SenUVK: Ein Back wird naturnah, https://www.berlin.de/sen/uvk/umwelt/wasser-und-geologie/europaeische-wasserrahmenrichtlinie/berlin/panke/, (last access: 19 Octoer 2023), 2009.

SenUVK: Wasserportal Gewässerkundliche Messdaten, Wasserportal Berlin [data set], https://wasserportal.berlin.de/start.php (last access: 29 September 2023), 2023.

Singh, J., Karmakar, S., Paimazumder, D., Ghosh, S., and Niyogi, D.: Urbanization alters rainfall extremes over the contiguous United States, Environ. Res. Lett., 15, 074033, https://doi.org/10.1088/1748-9326/ab8980, 2020.

Smith, A., Tetzlaff, D., Gelbrecht, J., L., K., and Soulsby, C.: Riparian wetland rehabibiltation and beaver re-colonisation impacts on hydrological processes and water quality in a lowland agricultural catchment, Sci. Total Environ., 699, 134302, https://doi.org/10.1016/j.scitotenv.2019.134302, 2020a.

Smith, A., Tetzlaff, D., Kleine, L., Maneta, M. P., and Soulsby, C.: Isotope-aided modelling of ecohydrologic fluxes and water ages under mixed land use in Central Europe: The 2018 drought and its recovery, Hydrol. Process., 34, 3406–3425, https://doi.org/10.1002/hyp.13838, 2020b.

Smith, A., Tetzlaff, D., Kleine, L., Maneta, M., and Soulsby, C.: Quantifying the effects of land use and model scale on water partitioning and water ages using tracer-aided ecohy-

drological models, Hydrol. Earth Syst. Sci., 25, 2239–2259, https://doi.org/10.5194/hess-25-2239-2021, 2021.

Smith, A. A., Tetzlaff, D., Maneta, M., and Soulsby, C.: Critical Zone Response Times and Water Age Relationships Under Variable Catchment Wetness States: Insights Using a Tracer-Aided Ecohydrological Model, Water Resour. Res., 58, e2021WR030584, https://doi.org/10.1029/2021WR030584, 2022.

Soulsby, C., Birkel, C., and Tetzlaff, D.: Assessing urbanization impacts on catchment transit times, Geophys. Res. Lett., 41, 442–448, https://doi.org/10.1002/2013GL058716, 2014.

Soulsby, C., Birkel, C., Geris, J., and Tetzlaff, D.: Spatial aggregation of time-variant stream water ages in urbanizing catchments, Hydrol. Process., 29, 3038–3050, https://doi.org/10.1002/hyp.10500, 2015.

Sprenger, M., Stumpp, C., Weiler, M., Aeschbach, W., Allen, S. T., Benettin, P., Dubbert, M., Hartmann, A., Hrachowitz, M., Kirchner, J. W., McDonnell, J. J., Orlowski, N., Penna, D., Pfahl, S., Rinderer, M., Rodriguez, N., Schmidt, M., and Werner, C.: The Demographics of Water: A Review of Water Ages in the Critical Zone, Rev. Geophys., 57, 800–834, https://doi.org/10.1029/2018RG000633, 2019.

Stevenson, J. L., Geris, J., Birkel, C., Tetzlaff, D., and Soulsby, C.: Assessing land use influences on isotopic variability and stream water ages in urbanising rural catchments, Isot. Environ. Healt. S., 58, 277–300, https://doi.org/10.1080/10256016.2022.2070615, 2022.

Stewardson, M. J., Acreman, M., Costelloe, J. F., Fletcher, T. D., Fowler, K. J. A., Horne, A. C., Liu, G., McClain, M. E., and Peel, M. C.: Chapter 3 – Understanding Hydrological Alteration, in: Water for the Environment, edited by: Horne, A. C., Webb, J. A., Stewardson, M. J., Richter, B., and Acreman, M., Academic Press, 37–64, https://doi.org/10.1016/B978-0-12-803907-6.00003-6, 2017.

Stewart, M. K., Morgenstern, U., and McDonnell, J. J.: Truncation of stream residence time: How the use of stable isotopes has skewed our concept of streamwater age and origin, Hydrol. Process., 24, 1646–1659, https://doi.org/10.1002/hyp.7576, 2010.

Tang, W. and Carey, S. K.: HydRun: A MATLAB toolbox for rainfall–runoff analysis, Hydrol. Process., 31, 2670–2682, https://doi.org/10.1002/hyp.11185, 2017.

Tetzlaff, D., Grottker, M., and Leibundgut, C.: Hydrological criteria to assess changes of flow dynamic in urban impacted catchments, Phys. Chem. Earth, 30, 426–431, https://doi.org/10.1016/j.pce.2005.06.008, 2005.

Tetzlaff, D., Soulsby, C., Hrachowitz, M., and Speed, M.: Relative influence of upland and lowland headwaters on the isotope hydrology and transit times of larger catchments, J. Hydrol., 400, 438–447, https://doi.org/10.1016/j.jhydrol.2011.01.053, 2011.

Tetzlaff, D., Buttle, J., Carey, S. K., Mcguire, K., Laudon, H., and Soulsby, C.: Tracer-based assessment of flow paths, storage and runoff generation in northern catchments: A review, Hydrol. Process., 29, 3475–3490, https://doi.org/10.1002/hyp.10412, 2015.

Tetzlaff, D., Smith, A., Kleine, L., Daempfling, H., Freymueller, J., and Soulsby, C.: Integrated ecohydrological hydrometric and stable water isotope data of a drought-sensitive mixed land use lowland catchment, Earth Syst. Sci. Data, 15, 1543–1554, https://doi.org/10.5194/essd-15-1543-2023, 2023.

Tonkin, J. D., Olden, J. D., Merritt, D. M., Reynolds, L. V., Rogosch, J. S., and Lytle, D. A.: Designing flow regimes to support entire river ecosystems, Front. Ecol. Environ., 19, 326–333, https://doi.org/10.1002/fee.2348, 2021.

Tramblay, Y., Rutkowska, A., Sauquet, E., Sefton, C., Laaha, G., Osuch, M., Albuquerque, T., Alves, M. H., Banasik, K., Beaufort, A., Brocca, L., Camici, S., Csabai, Z., Dakhlaoui, H., DeGirolamo, A. M., Dörflinger, G., Gallart, F., Gauster, T., Hanich, L., Kohnová, S., Mediero, L., Plamen, N., Parry, S., Quintana-Seguí, P., Tzoraki, O., and Datry, T.: Trends in flow intermittence for European rivers, Hydrol. Sci. J., 66, 37–49, https://doi.org/10.1080/02626667.2020.1849708, 2021.

Umweltatlas Berlin/ALKIS: FIS-Broker, https://fbinter.stadt-berlin.de/fb/index.jsp (last access: 12 September 2023), 2020.

Van Loon, A. F. and Laaha, G.: Hydrological drought severity explained by climate and catchment characteristics, J. Hydrol., 526, 3–14, https://doi.org/10.1016/j.jhydrol.2014.10.059, 2015.

von Freyberg, J., Allen, S. T., Seeger, S., Weiler, M., and Kirchner, J. W.: Sensitivity of young water fractions to hydro-climatic forcing and landscape properties across 22 Swiss catchments, Hydrol. Earth Syst. Sci., 22, 3841–3861, https://doi.org/10.5194/hess-22-3841-2018, 2018.

Wallace, S., Biggs, T., Lai, C. T., and McMillan, H.: Tracing sources of stormflow and groundwater recharge in an urban, semi-arid watershed using stable isotopes, J. Hydrol. Reg. Stud., 34, 100806, https://doi.org/10.1016/j.ejrh.2021.100806, 2021.

Warter, M. M.: Inter-catchment comparison between an urban and rural agricultural stream, FRED [data set], https://doi.org/10.18728/igb-fred-865.0, 2024.

Warter, M. M., Tetzlaff, D., Ring, A. M., Christopher, J., Kissener, H. L., Funke, E., Sparmann, S., Mbedi, S., Soulsby, C., and Monaghan, M. T.: Environmental DNA, hydrochemistry and stable water isotopes as integrative tracers of urban ecohydrology, Water Res., 250, 121065, https://doi.org/10.1016/j.watres.2023.121065, 2024.

Weiler, M., McGlynn, B. L., McGuire, K. J., and McDonnell, J. J.: How does rainfall become runoff? A combined tracer and runoff transfer function approach, Water Resour. Res., 39, 1315, https://doi.org/10.1029/2003WR002331, 2003.

Wu, S., Tetzlaff, D., Goldhammer, T., and Soulsby, C.: Hydroclimatic variability and riparian wetland restoration control the hydrology and nutrient fluxes in a lowland agricultural catchment, J. Hydrol., 603, 126904, https://doi.org/10.1016/j.jhydrol.2021.126904, 2021.

Wunsch, A., Liesch, T., and Broda, S.: Deep learning shows declining groundwater levels in Germany until 2100 due to climate change, Nat. Commun., 13, 1–13, https://doi.org/10.1038/s41467-022-28770-2, 2022.

Yang, G., Bowling, L. C., Cherkauer, K. A., and Pijanowski, B. C.: The impact of urban development on hydrologic regime from catchment to basin scales, Landscape Urban Plan., 103, 237–247, https://doi.org/10.1016/j.landurbplan.2011.08.003, 2011.

Ying, Z., Tetzlaff, D., Freymueller, J., Comte, J. C., Goldhammer, T., Schmidt, A., and Soulsby, C.: Developing a conceptual model of groundwater – Surface water interactions in a drought sensitive lowland catchment using multi-proxy data, J. Hydrol., 628, 130550, https://doi.org/10.1016/j.jhydrol.2023.130550, 2024.

Nat. Hazards Earth Syst. Sci., 24, 3907–3924, 2024

https://doi.org/10.5194/nhess-24-3907-2024